



OPEN

Predictive value of PET metabolic parameters for occult lymph node metastases in PET/CT defined node-negative patients with advanced epithelial ovarian cancer

Bing Xue¹ & Xihai Wang²✉

Accurate lymph node metastasis (LNM) prediction is crucial for patients with advanced epithelial ovarian cancer (AEOC) since it guides the decisions about lymphadenectomy. Previous studies have shown that occult lymph node metastasis (OLNM) is common in AEOC. The objective of our study is to quantitatively assess the probability of occult lymph node metastasis defined by ¹⁸F-Fluorodeoxyglucose PET/CT in AEOC and explore relationship between OLNM and PET metabolic parameters. The patients with pathologically confirmed AEOC who underwent PET/CT for preoperative staging at our institute were reviewed. Univariate and multivariate analysis were performed to evaluate the predictive value of PET/CT-related metabolic parameters for OLNM. The result of our study showed metastatic TLG index had a better diagnostic performance than other PET/CT-related metabolic parameters. Two variables were independently and significantly associated with OLNM in multivariate analysis: metastatic TLG index and primary tumor location. The logistic model combining metastatic TLG index, primary tumor location, and CA125 might be a promising tool to effectively predict the individualized possibility of OLNM for AEOC patients.

Ovarian carcinoma is one of the deadliest gynecologic cancers because the majority of patients are diagnosed with advanced-stage (stage III and IV) according to the International Federation of Gynecology and Obstetrics (FIGO) staging classification¹. Epithelial ovarian cancer (EOC) is the most crucial histological subtype, accounting for approximately 70% of ovarian cancers^{2,3}. Lymph node (LN) status has an important impact on the FIGO stage of EOC^{4,5}. Although debulking surgery is the standard treatment of AEOC, pelvic and para-aortic lymphadenectomy is not necessary for all patients⁶. Studies have shown no benefit in overall survival or progression-free survival between cytoreductive surgery with and without pelvic and para-aortic lymphadenectomy, suggesting that lymphadenectomy should be omitted for those patients without LNM^{7,8}. Identification of metastatic LN in patients with AEOC before debulking surgery is important as it guides decisions about lymphadenectomy.

The frequency of LNM observed in EOC is up to 75% of patients with stage III–IV and 25% of patients with stage I–II^{8,9}. LNM has been evaluated using several non-invasive modalities of preoperative imaging, such as computed tomography (CT), magnetic resonance imaging (MRI), and 2-[¹⁸F] fluoro-2-deoxy-D-glucose (¹⁸F-FDG) PET/CT^{10–13}. Clinical OLNM is defined as no suspicion of lymph node involvement on CT or PET images¹⁴. In prior studies, OLNM was mainly defined according to CT modality. However, PET/CT, which can provide the functional and anatomical information of malignancy, is considered the most accurate LNM staging modality^{15–17}. Although preoperative PET/CT showed higher diagnostic accuracy than CT in detecting pelvic and para-aortic LNM in AEOC, the sensitivity of PET/CT was unsatisfactory, ranging from 26.7 to 87.6%^{18–20}. Low diagnostic sensitivity of PET/CT indicated clinical OLNM was common for AEOC, which accounted for approximately 20–80% of patients^{10,16,18}.

¹Department of Nuclear Medicine, The Fourth Affiliated Hospital of China Medical University, Shenyang 110032, China. ²Department of Radiology, Shengjing Hospital of China Medical University, Shenyang 110004, China. ✉email: wang052235@hotmail.com

Therefore, the challenge is to distinguish the patients with OLNLM who should have a lymphadenectomy from the patients with “no suspicious lymph nodes” who should not have lymphadenectomy. Previous studies have demonstrated that certain PET/CT parameters, such as standardized uptake value (SUV), metabolic tumor volume (MTV), and total lesion glycolysis (TLG), were significant prognostic factors for AEOC^{21–25}. The SUV is a ratio of radioactivity concentration in tissue at a point in time divided by the injected dose of radioactivity per kilogram of the patient’s weight, which is a simple way of determining activity in PET imaging. MTV refers to the metabolically active volume of the tumor segmented using FDG PET, and has been shown to be useful in predicting patient outcome and in assessing treatment response. However, there was no study to evaluate the correlation between PET/CT-related parameters and LNM, especially OLNLM. Previous studies have demonstrated that hypermetabolic LN on PET/CT, initial CA125 ≥ 500 , and initial peritoneal cancer index (PCI) ≥ 10 were independently and significantly associated with pelvic and/or para-aortic LNM^{26,27}. Recently, many researchers have focused on radiomics features of PET/CT or contrast-enhanced CT in predicting LNM in AEOC, among which LNM assessment has been proven to have a certain significant improvement^{28,29}. However, the manually time-consuming delineation of region of interesting (ROI) and complex models limit its clinical application. The objective of our study is to evaluate the relationship between PET/CT-related parameters and OLNLM and construct a simple model to predict OLNLM.

Materials and methods

Patients. The study was conducted in accordance with the Declaration of Helsinki (as revised in 2013). This retrospective study was approved by the medical ethics committee of Shengjing Hospital of China Medical University (2020PS374K). Informed consent was not required by medical ethics committee of Shengjing Hospital of China Medical University due to the retrospective nature of the study.

From January 2013 to December 2022, a total of 777 consecutive patients with pathologically confirmed EOC who underwent ¹⁸F-FDG PET/CT for preoperative staging at our institute were reviewed. Inclusion criteria were as follows: (1) received debulking surgery with pelvic and para-aortic lymphadenectomy; (2) postoperative pathological examination confirmed stage III or IV EOC with definite LN status; (3) PET/CT scan was performed within one month before surgery. The exclusion criteria included the following: (1) received any neoadjuvant chemotherapy (NAC) before surgery; (2) poor image quality or image data loss; (3) negative uptake of the primary or metastatic lesions in PET/CT images (SUV_{max} < 2.5).

The PET/CT images of patients who met the inclusion criteria were evaluated by two radiologists (with more than 5 years of experience in abdominal imaging of PET/CT images) to confirm presence of positive LN on PET/CT images. Further analysis was performed for the patients with no positive LN on PET/CT, and those patients were categorized into two groups based on postoperative pathological findings: those with LNM (OLNLM) and those without any LN involvement (NLNLM). The patients with positive LN on PET/CT images were not further analyzed.

The flowchart of patient selection is shown in Fig. 1.

Clinical data such as age, menopause status, CA125 and so on were collected from the hospital information system of our hospital. The ascites and location of primary tumor were evaluated by previous radiologists on PET/CT scans. The ascitic volume was divided into two categories: small (< 1500 ml) and large amount of ascitic (≥ 1500 ml), according to ascitic volume assessed on CT component of PET/CT³⁰. The classification of ascites volume is based on our clinical experience and previous studies³¹. FDG avid in one side or two side tubo-ovarian was defined as unilateral or bilateral involvement.

LN status assessment. In our study, the procedures for LN dissection included pelvic lymphadenectomy and para-aortic lymphadenectomy. The extent of LN dissection included seven subregions: para-aortic, common iliac, lateral sacral, external iliac, internal iliac (hypogastric), obturator, and inguinal. The LN dissection and postoperative pathological results were classified by subregion. Our study defined LNM as confirmed involvement of one or more of the above subregions based on postoperative pathological results. The preoperative LN status on PET/CT images of enrolled patients was evaluated by two radiologists according to the seven subregions (Fig. 2). Inconsistent results were resolved through consultation by the two radiologists. OLNLM was defined as postoperative pathological confirmation of LNM with no suspicion of LN involvement on either CT (short-axis diameter < 1 cm) or PET (SUV_{max} < 2.5).

¹⁸F-FDG PET/CT image acquisition. Whole-body ¹⁸F-FDG PET/CT scans were performed using a dedicated PET/CT scanner (Discovery 690, GE Healthcare, Milwaukee, WI) within one month before any treatment. Patients fasted for at least 6 h and were injected with 3.7 MBq/kg \pm 10% of body weight ¹⁸F-FDG. The fasting serum glucose and insulin injection were strictly controlled. Patients with uncontrolled diabetes or hyperglycemia may require rescheduling of the scan to avoid inaccurate results. Then the acquisition was performed after approximately 60 min. The 3D ordered subset expectation maximization (OSEM) algorithm with attenuation correction was used for the reconstruction of the PET image. The voxel sizes of the reconstructed PET image were 3.65 \times 3.65 \times 3.27 mm³, and the matrix size was 192 \times 192. CT scans (109 mA, 140 kV) were performed before the PET scan with a matrix size of 512 \times 512 and a voxel size of 0.98 \times 0.98 \times 3.75 mm³.

Measurement of PET metabolic parameters. Finally, PET/CT images were imported into 3D Slicer software (version 4.8.1, <https://www.slicer.org/>) to extract PET metabolic parameters. The PETTumorSegmentation extension within 3D Slicer was used to delineate primary and metastatic lesions, providing an editor-effect for semi-automated segmentation of tumors and hot lymph nodes in PET scans³². Multiple areas were selected as ROI. To avoid including physiologic uptake in the volume of interest, a combined CT and PET scan reading

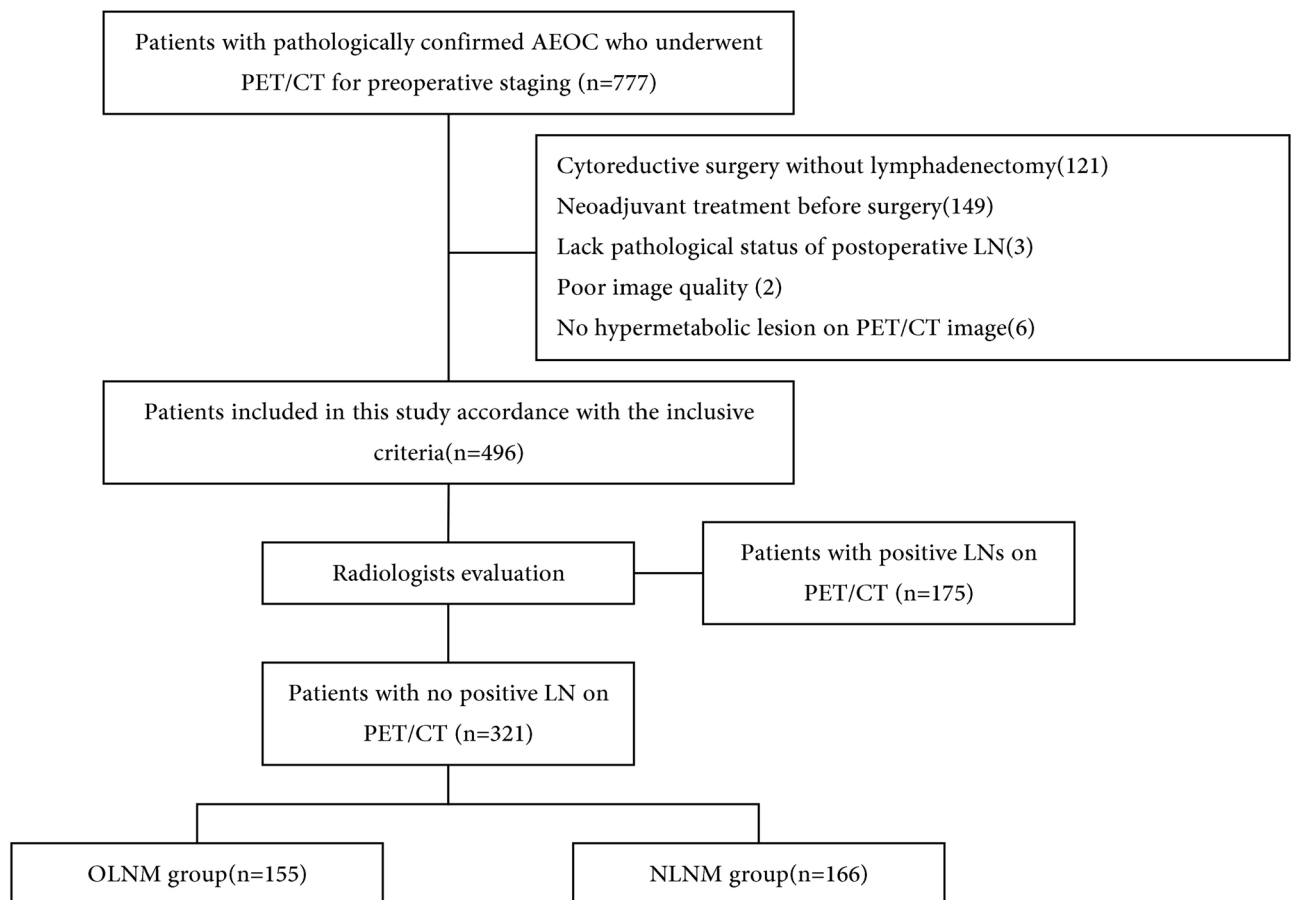


Figure 1. Flow chart of patient selection.

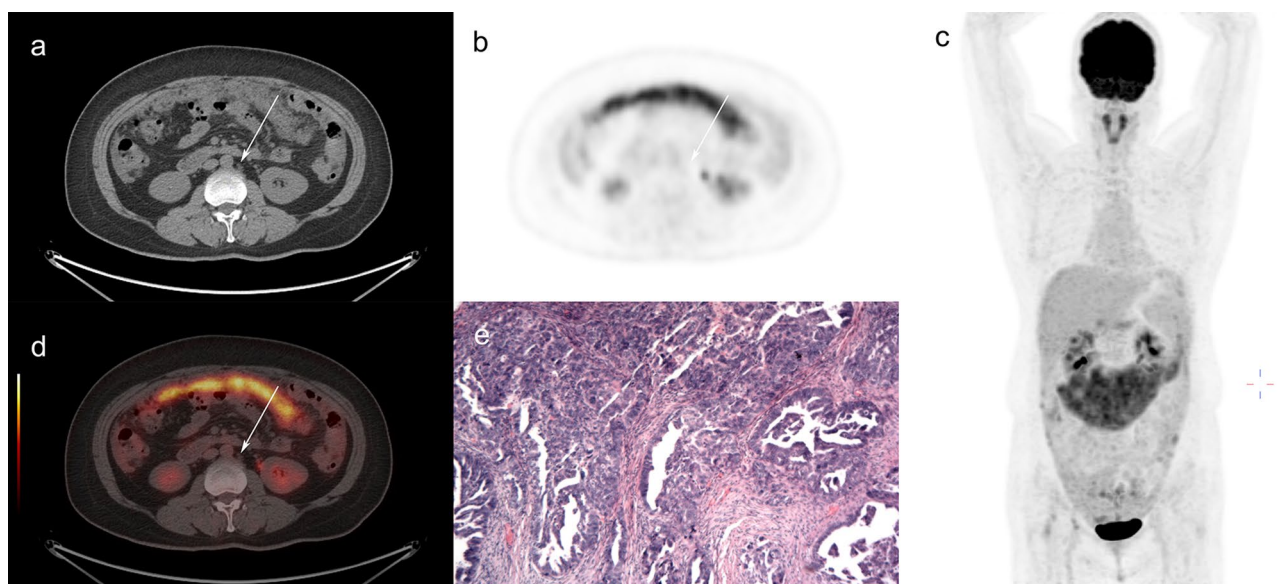


Figure 2. A 42-year-old female with pathologically diagnosed high-grade serous carcinoma. Pelvic and para-aortic lymph node metastasis were confirmed by postoperative pathological results. There were small para-aortic lymph nodes presented in the lymph draining area on CT scan (a). However, no FDG avid in those lymph nodes on maximum intensity projection (b, c) and fused PET/CT (d) images. The postoperative pathological results confirmed lymph node metastasis of high-grade serous carcinoma, HE staining, magnification 100× (e). The metastatic MTV and TLG index of this patient was 96.2% and 97.5%, respectively.

was performed. PET-IndiC, another extension of 3D Slicer, was used to calculate PET-related metabolic parameters. The following parameters were measured in primary and all lesions: SUV_{mean}, SUV_{max}, MTV, TLG, and SUV_{peak}. The SUV_{max} was determined as the maximum value in multiple ROIs. MTV or TLG was calculated as the sum of each ROI, while SUV_{mean} and SUV_{peak} were determined as the mean of each ROI. The MTV and TLG of metastatic lesions were calculated by subtracting the values of primary lesions from those of all lesions. The proportion of MTV and TLG of metastatic lesions in relation to all lesions were defined as the metastatic MTV index and metastatic TLG index, respectively.

$$\text{Metastatic MTV index} = \frac{\text{MTV metastases}}{\text{MTV all lesions}} \times 100\%$$

$$\text{Metastatic TLG index} = \frac{\text{TLG metastases}}{\text{TLG all lesions}} \times 100\%$$

Statistical analysis. Student t-tests or Mann–Whitney U tests were used for continuous variables, and Chi-squared tests and exact Fisher tests were applied for categorical variables between two groups. The association between variables and OLN was evaluated by univariate logistic regression analysis. The features with a p value < 0.05 in the univariate logistic regression analysis were selected for multivariate logistic regression analysis. The multivariate logistic regression analysis with the optimal subset method was used to assess the best combination of variables that were independently associated with OLN. The ROC curve was used to assess the performance of the final logistic model. All analysis and calculations were done with R (version 4.0.5, www.Rproject.org). A p value < 0.05 was considered statistically significant.

Ethics approval and content to participate. Ethics approval was granted by the ethics committee of the Shengjing Hospital of China Medical University.

Result

Patient selection and clinical characteristics. Our study included 496 patients with primary AEOC who met all inclusion criteria. Among them, 175 patients showing positive LNs on PET/CT images were excluded. Finally, 321 patients who were evaluated by radiologists and showed no positive LN on PET/CT images were divided into OLN group ($n = 155$) and the NLNM group ($n = 166$). OLN accounted for 51.3% of all LNM and 48.3% of negative LN on PET/CT scans. The characteristics of the patients for further analysis are shown in Table 1. In the OLN group, 48 patients were associated with both pelvic and para-aortic LNM, 86 patients only had pelvic LNM, and 21 patients only had para-aortic LNM. There was no significant difference in the number of LNs resected in cytoreductive surgery, 20.434 ± 10.543 in the NLNM group and 21.987 ± 12.210 in the OLN group. The age, initial HE4, initial CA125, and menopausal state showed no statistically significant difference between two groups.

Predictive performance of PET metabolic parameters. The results of univariate logistic regression analysis of PET-related metabolic parameters showed MTV of primary lesions, TLG of primary lesions, MTV of all lesions, MTV of metastatic lesions, metastatic MTV index, and metastatic TLG index were significantly associated with OLN. In ROC curve analysis, the AUC of metastatic TLG index (0.684, 95% CI 0.645–0.760) was larger than other PET-related metastatic parameters (Fig. 3). We found severe collinearity between PET-related metabolic parameters with $p < 0.05$ in univariate analysis. The correlation between those parameters was assessed by Pearson correlation analysis (Table 2).

Risk factors and prediction model. Among all clinical characteristics, the volume of ascites, CA125, and location of the primary tumor were significantly correlated with a high risk of OLN ($p < 0.05$). To eliminate the correlation and multiple linearities between the variables, particularly PET-related metabolic parameters, multivariate logistic regression with an optimum subset method was utilized to simplify the financial indexes. The findings from the univariate and multivariate logistic analysis are presented in Table 3. The metastatic TLG index (OR = 4.740, 95% CI 2.453–9.320) and location of primary tumors (OR = 1.930, 95% CI 1.074–3.531) were significantly associated with OLN ($p < 0.05$) in multivariate logistic analysis. The results are displayed using forest plots (Fig. 4). The ROC-AUC of the final logistic model after bootstrap replicates 1000 times was 0.702 (95% CI 0.645–0.759) (Fig. 5a). The predicted and observed probabilities of OLN is shown in Fig. 5b and do not differ significantly ($p = 0.06$).

Discussion

The state of LN in patients with AEOC affects the choice of lymphadenectomy and prognosis³³. This was the first clinical study to assess occult pelvic and para-aortic LNM in patients with AEOC after cytoreductive surgery. In our study, the proportion of clinical OLN was high, accounting for 51.3% of all LNM and 48.3% of negative LN on PET/CT scans. The primary tumor location and metastatic TLG index extracted from TLG of metastatic and all lesions were significantly associated with OLN. The final logistic model could predict OLN in AEOC before surgery.

The use of systematic lymphadenectomy is controversial for patients with EOC. Although the positive rate of lymph nodes in patients with presumed early-stage EOC was low (appropriately 3–14% detected by systematic lymphadenectomy), LNM in AEOC was high^{4,5,34}. LNM was found in 60.9% of all patients in our study, similar

Characteristics	NLNM group n = 166	OLNM group n = 155	P value
Age	55.825 ± 9.660	54.245 ± 9.271	0.136
Ascites			0.005
Small	111 (66.867%)	79 (50.968%)	
Large	55 (33.133%)	76 (49.032%)	
HE4	524.233 ± 405.548	618.708 ± 409.960	0.039
CA199	67.658 ± 168.730	33.129 ± 81.675	0.019
CA724	43.803 ± 72.517	63.302 ± 91.523	0.036
CA125	1067.805 ± 1264.763	1461.316 ± 1479.211	0.011
Pathological type			0.069
HGSOC	136 (81.928%)	139 (89.677%)	
Others	30 (18.072%)	16 (10.323%)	
Menopausal state			0.453
No	41 (24.699%)	45 (29.032%)	
Yes	125 (75.301%)	110 (70.968%)	
Resected LN numbers	20.434 ± 10.543	21.987 ± 12.210	0.223
Resected LN stations	0.000 ± 0.000	4.000 ± 4.218	< 0.001
Location			0.001
Unilateral	51 (30.723%)	22 (14.194%)	
Bilateral	115 (69.277%)	133 (85.806%)	
Primary lesions SUVmean	6.409 ± 2.603	6.394 ± 4.145	0.969
Primary lesions SUVmax	15.786 ± 7.022	15.267 ± 13.879	0.676
Primary lesions MTV	174.514 ± 163.401	128.518 ± 130.195	0.005
Primary lesions TLG	1196.512 ± 1326.612	821.808 ± 871.071	0.003
Primary lesions SUVpeak	12.936 ± 6.067	11.947 ± 8.602	0.238
All lesions SUVmean	6.193 ± 2.497	5.814 ± 2.079	0.14
All lesions SUVmax	17.497 ± 11.131	17.226 ± 17.489	0.87
ALL lesion MTV	311.310 ± 255.478	385.207 ± 292.735	0.016
ALL lesion TLG	2016.447 ± 2019.289	2347.499 ± 2181.457	0.159
ALL lesion SUVpeak	13.824 ± 6.860	19.437 ± 54.441	0.204
Metastatic lesions MTV	136.792 ± 232.498	251.595 ± 264.120	< 0.001
Metastatic MTV index	0.355 ± 0.351	0.577 ± 0.341	< 0.001
Metastatic lesions TLG	819.936 ± 1512.754	1478.419 ± 1774.855	< 0.001
Metastatic TLG index	0.334 ± 0.351	0.559 ± 0.343	< 0.001

Table 1. Patients characteristics.

to the previous studies⁹. Occult nodal involvements were frequently found in AEOC. In our study, only 48.75% of the cases with LNM had positive lymph nodes on PET/CT scans. The other 51.25% of cases were negative on PET/CT scans. ¹⁸F-FDG PET/CT is the most accurate modality for preoperative tumor staging and detection of metastatic lymph nodes. A high proportion of LNM is negative in PET/CT scans due to the low spatial resolution of PET-CT images and the low tissue uptake of the ¹⁸F-FDG. Most of the metastatic lesions, including LNM, tends to uptake less FDG than primary lesions. Furthermore, tumor FDG binding depends on histological type and has a low affinity in mucus and clear cell adenocarcinoma³⁵. In addition, the micro-metastases will not be detected due to the low reconstructed spatial resolution of PET. A previous study demonstrated sensitivity for detecting metastatic lesions 4 mm or less in short-axis diameter was 12.5%, and for between 5 and 9 mm was 66.7%³⁶. Finally, massive ascites and extensive peritoneal metastasis also limit the detection of LNM on PET/CT scans. In summary, OLNLM is frequently observed in AEOC, which leads to the low sensitivity of PET/CT for LNM evaluation.

Many previous studies demonstrated that it was feasible to improve the diagnostic efficiency in LNM by clinical factors, radiological findings, and radiomics features extracted from PET or CT images. A new diagnostic tool based on multivariate analysis, including three variables—pelvic and/or para-aortic LNM on CT PET/CT, initial PCI ≥ 10, and initial CA125 ≥ 500—was proposed²⁷. Another study used preoperative radiological scores to predict pelvic and/or para-aortic LNM²⁸. Although the ROC-AUC of those prediction models were moderate, the preoperative assessment of PCI/or colon involvement was difficult and ambiguous. Many studies have demonstrated the value of radiomics features in predicting LNM of EOC^{28,37}. The radiomics signatures extracted from CT images incorporating LN reports by radiologists could improve the diagnostic efficiency in LNM³⁷. However, the calculation of the radiomics features is very complicated and time-consuming. We also found that the evaluation of LNM mainly relied on the subjective assessment of LNM by radiologists in previous studies.

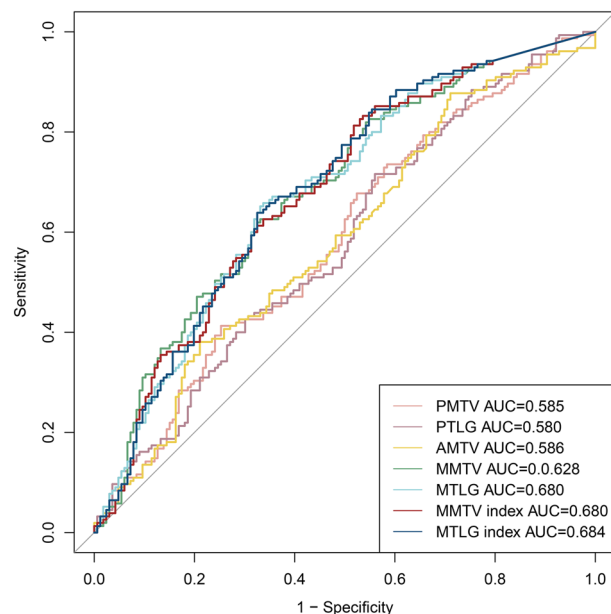


Figure 3. ROC curves of PET-related metabolic parameters for OLN.

Variables	Primary lesions MTV	Primary lesions TLG	ALL lesion MTV	Metastatic lesions MTV	Metastatic MTV index	Metastatic lesions TLG	Metastatic TLG index
Primary lesions MTV	1.000	0.849	0.352	-0.217	-0.560	-0.163	-0.556
Primary lesions TLG	0.849	1.000	0.345	-0.142	-0.444	-0.038	-0.457
ALL lesion MTV	0.352	0.345	1.000	0.824	0.343	0.802	0.348
Metastatic lesions MTV	-0.217	-0.142	0.824	1.000	0.692	0.941	0.695
Metastatic MTV index	-0.560	-0.444	0.343	0.692	1.000	0.615	0.990
Metastatic lesions TLG	-0.163	-0.038	0.802	0.941	0.615	1.000	0.623
Metastatic TLG index	-0.556	-0.457	0.348	0.695	0.990	0.623	1.000

Table 2. Pearson correlation of the PET/CT parameters with $p < 0.05$ in univariate analysis.

It is easy to identify positive LN on PET/CT scans because of hypermetabolism of metastatic LN. Identification of OLN is critical for improving sensitivity in detecting LNM.

Previous studies have investigated the predictive value of PET metabolic parameters in AEOC^{25,27,31}. MTV and TLG were found to be independent prognostic factors for disease progression and overall survival after cytoreductive surgery in patients with EOC^{23,25}. In our study, MTV, TLG, metastatic TLG index, and metastatic MTV index were highly associated with OLN. The metastatic TLG index was the only independent predictive factor in both univariate and multivariate analysis and had a higher predictive value than other PET-related parameters. The metastatic TLG and MTV indexes can quantify EOC's metastatic capacity, which positively correlate with metastatic tumor burden. OLN, as part of metastatic lesions, was closely associated with soakage and metastasis of malignant ovarian tumors.

The metastatic TLG index had a better AUC (0.684) compared to other PET metabolic parameters. However, combining clinical features can significantly improve the predictive ability of OLN. In this study, the final multivariate model incorporated CA125, bilateral ovarian involvement, and metastatic TLG index. Bilateral ovarian cancers were found to be associated with a higher risk of OLN due to increased tumor heterogeneity and invasiveness. Although CA125 was not an independent predictive factor in the multivariate analysis, it plays an important role in ovarian cancer diagnosis and follow-up.

There are several limitations to the present study. Firstly, this study is a retrospective analysis conducted at a single center, which may potentially suffer from inherent selection bias and limit the generalizability of the data. All patients underwent PET/CT scans using the same devices at our hospitals. However, the resolution of the images, administration of a carbohydrate-free diet before scanning, and time for uptake were inevitably different, which may have resulted in heterogeneous results. Further multicenter studies are necessary to confirm the efficiency of the results of this study. Secondly, our study only used PET/CT to predict OLN. Although PET/CT is the most accurate imaging modality for detecting LNM, a comparison of PET/CT with contrast-enhanced CT or MRI for OLN will be necessary in further studies. Thirdly, our study focused on patients with negative

Variables	Univariate analysis		Multivariate analysis	
	OR (95% CI)	P	OR (95% CI)	P
Age	0.982(0.959,1.005)	0.137		
Ascites (Small/Large)	1.941(1.239,3.059)	0.004		
CA199	0.997(0.995, 0.999)	0.036		
HE4	1.000(0.999,1.000)	0.314		
CA724	1.002(1.000,1.005)	0.053		
CA125	1.000(1.000,1.000)	0.012	1.000(1.000–1.000)	0.104
Menopausal state (Yes/No)	0.802(0.488,1.315)	0.381		
Pathological (HGSOC/Others)	0.521(0.266,0.988)	0.05		
Location (Unilateral/Bilateral)	2.681(1.550,4.761)	0.001	1.930(1.074–3.531)	0.03
Primary lesions SUVmean	0.998(0.931,1.068)	0.968		
Primary lesions SUVmax	0.995(0.970,1.016)	0.673		
Primary lesions MTV	0.997(0.996,0.999)	0.007		
Primary lesions TLG	0.999(0.999,0.999)	0.005		
Primary lesions SUVpeak	0.980(0.942,1.011)	0.264		
All lesions SUVmean	0.928(0.834,1.023)	0.148		
All lesions SUVmax	0.998(0.981,1.014)	0.867		
ALL lesions MTV	1.001(1.000,1.001)	0.019		
ALL lesions TLG	1.000(0.999,1.000)	0.163		
ALL lesions SUVpeak	1.004(0.996,1.025)	0.451		
Metastatic lesions MTV	1.004(1.002,1.007)	<0.001		
Metastatic MTV index	5.801(3.069,11.19)	<0.001		
Metastatic lesions TLG	1.001(0.999,1.004)	0.156		
Metastatic TLG index	5.908(3.129,11.39)	<0.001	4.740(2.453–9.320)	<0.001

Table 3. Univariate and multivariate logistic analysis for OLNLM.

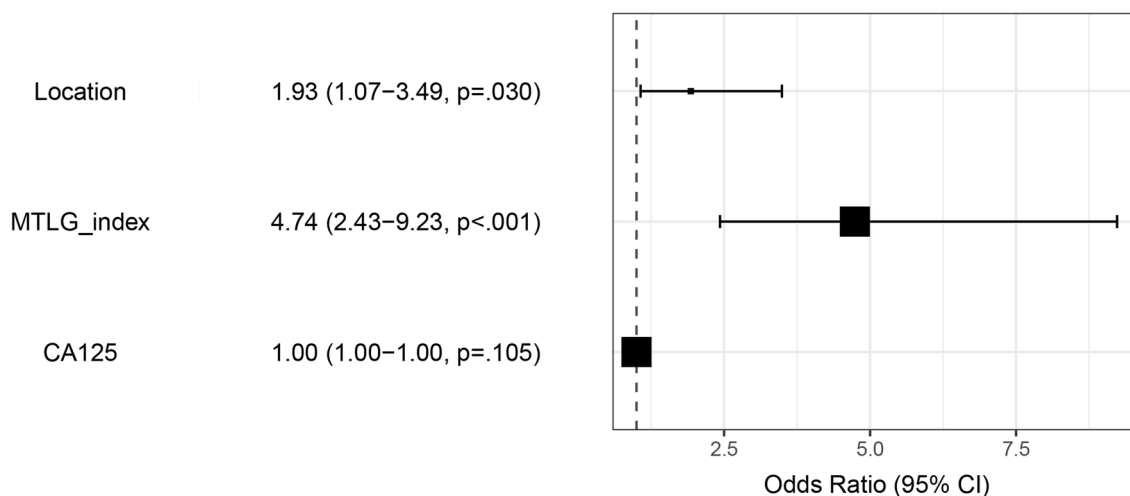


Figure 4. The display of multivariate logistic regression using forest plot.

LN on PET/CT scans. Only the patients with negative reports in PET/CT scans were included in our study. A comparison between OLNLM and pathologically confirmed no LNM, regardless of positive LN on PET/CT, will be needed in further studies.

Conclusions

In conclusion, our study demonstrated that OLNLM defined by PET/CT was frequently observed in patients with AEOC. The metastatic TLG index extracted from metastatic and all hot lesions was found to be a significant predictor of OLNLM. The logistic model, which combines the metastatic TLG index, primary tumor location, and CA125 is a promising tool for improving the diagnostic accuracy of OLNLM. Hence, this simple method may provide valuable information for triaging patients according to simple lymphadenectomy decision rules.

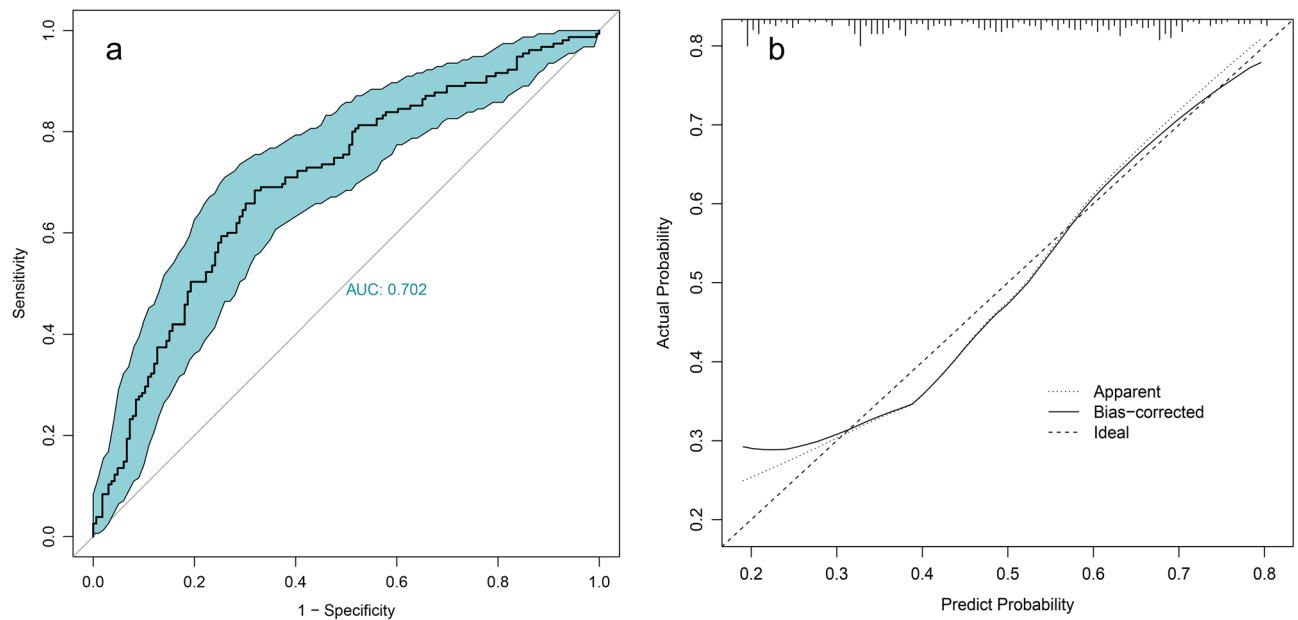


Figure 5. Internal calibration of the final logistic regression model. ROC curve of the logistic regression model (a) with bootstrap 1000 times, Calibration curve with the Hosmer–Lemeshow test (b).

Data availability

The datasets used and/or analyzed during the current study are available from the corresponding author on reasonable request.

Received: 15 March 2023; Accepted: 7 June 2023

Published online: 09 June 2023

References

1. Akbulut, S. *et al.* Hydatid cyst of the pancreas: Report of an undiagnosed case of pancreatic hydatid cyst and brief literature review. *World J. Gastrointest. Surg.* **6**, 190–200. <https://doi.org/10.4240/wjgs.v6.i10.190> (2014).
2. Ledermann, J. A. *et al.* Newly diagnosed and relapsed epithelial ovarian carcinoma: ESMO Clinical Practice Guidelines for diagnosis, treatment and follow-up. *Ann Oncol* **29**, iv259. <https://doi.org/10.1093/annonc/mdy157> (2018).
3. Lavoue, V. *et al.* Management of epithelial cancer of the ovary, fallopian tube, and primary peritoneum. Long text of the Joint French Clinical Practice Guidelines issued by FRANCOGYN, CNGOF, SFOG, and GINECO-ARCAGY, and endorsed by INCa. Part 1: Diagnostic exploration and staging, surgery, perioperative care, and pathology. *J. Gynecol. Obstet. Hum. Reprod.* **48**, 369–378. <https://doi.org/10.1016/j.jogoh.2019.03.017> (2019).
4. Pereira, A., Magrina, J. F., Rey, V., Cortes, M. & Magtibay, P. M. Pelvic and aortic lymph node metastasis in epithelial ovarian cancer. *Gynecol. Oncol.* **105**, 604–608. <https://doi.org/10.1016/j.ygyno.2007.01.028> (2007).
5. Walter, A. J. & Magrina, J. F. Contralateral pelvic and aortic lymph node metastasis in clinical stage I epithelial ovarian cancer. *Gynecol. Oncol.* **74**, 128–129. <https://doi.org/10.1006/gyno.1999.5370> (1999).
6. du Bois, A. *et al.* Potential role of lymphadenectomy in advanced ovarian cancer: A combined exploratory analysis of three prospectively randomized phase III multicenter trials. *J. Clin. Oncol.* **28**, 1733–1739. <https://doi.org/10.1200/JCO.2009.25.3617> (2010).
7. Harter, P. *et al.* A randomized trial of lymphadenectomy in patients with advanced ovarian neoplasms. *N. Engl. J. Med.* **380**, 822–832. <https://doi.org/10.1056/NEJMoa1808424> (2019).
8. Bachmann, C., Bachmann, R., Fend, F. & Wallwiener, D. Incidence and impact of lymph node metastases in advanced ovarian cancer: Implications for surgical treatment. *J. Cancer* **7**, 2241–2246. <https://doi.org/10.7150/jca.15644> (2016).
9. Morice, P. *et al.* Lymph node involvement in epithelial ovarian cancer: Analysis of 276 pelvic and paraaortic lymphadenectomies and surgical implications. *J. Am. Coll. Surg.* **197**, 198–205. [https://doi.org/10.1016/S1072-7515\(03\)00234-5](https://doi.org/10.1016/S1072-7515(03)00234-5) (2003).
10. Yuan, Y., Gu, Z. X., Tao, X. F. & Liu, S. Y. Computer tomography, magnetic resonance imaging, and positron emission tomography or positron emission tomography/computer tomography for detection of metastatic lymph nodes in patients with ovarian cancer: A meta-analysis. *Eur. J. Radiol.* **81**, 1002–1006. <https://doi.org/10.1016/j.ejrad.2011.01.112> (2012).
11. Khiewvan, B. *et al.* An update on the role of PET/CT and PET/MRI in ovarian cancer. *Eur. J. Nucl. Med. Mol. Imaging* **44**, 1079–1091. <https://doi.org/10.1007/s00259-017-3638-z> (2017).
12. Caobelli, F. *et al.* Predictive value of (18)F-FDG PET/CT in restaging patients affected by ovarian carcinoma: A multicentre study. *Eur. J. Nucl. Med. Mol. Imaging* **43**, 404–413. <https://doi.org/10.1007/s00259-015-3184-5> (2016).
13. Kitajima, K. *et al.* Preoperative risk stratification using metabolic parameters of (18)F-FDG PET/CT in patients with endometrial cancer. *Eur. J. Nucl. Med. Mol. Imaging* **42**, 1268–1275. <https://doi.org/10.1007/s00259-015-3037-2> (2015).
14. Deng, J. *et al.* Lung cancer with PET/CT-defined occult nodal metastasis yields favourable prognosis and benefits from adjuvant therapy: A multicentre study. *Eur. J. Nucl. Med. Mol. Imaging* **49**, 2414–2424. <https://doi.org/10.1007/s00259-022-05690-3> (2022).
15. Nam, E. J. *et al.* Diagnosis and staging of primary ovarian cancer: Correlation between PET/CT, Doppler US, and CT or MRI. *Gynecol. Oncol.* **116**, 389–394. <https://doi.org/10.1016/j.ygyno.2009.10.059> (2010).
16. Kitajima, K. *et al.* Diagnostic accuracy of integrated FDG-PET/contrast-enhanced CT in staging ovarian cancer: Comparison with enhanced CT. *Eur. J. Nucl. Med. Mol. Imaging* **35**, 1912–1920. <https://doi.org/10.1007/s00259-008-0890-2> (2008).
17. Yoshida, Y. *et al.* Incremental benefits of FDG positron emission tomography over CT alone for the preoperative staging of ovarian cancer. *AJR Am. J. Roentgenol.* **182**, 227–233. <https://doi.org/10.2214/ajr.182.1.1820227> (2004).

18. Tardieu, A. *et al.* Assessment of lymph node involvement with PET-CT in advanced epithelial ovarian cancer. A FRANCOGYN group study. *J. Clin. Med.* <https://doi.org/10.3390/jcm10040602> (2021).
19. Signorelli, M. *et al.* Detection of nodal metastases by 18F-FDG PET/CT in apparent early stage ovarian cancer: A prospective study. *Gynecol. Oncol.* **131**, 395–399. <https://doi.org/10.1016/j.ygyno.2013.08.022> (2013).
20. Hynninen, J. *et al.* FDG PET/CT in staging of advanced epithelial ovarian cancer: Frequency of supradiaphragmatic lymph node metastasis challenges the traditional pattern of disease spread. *Gynecol. Oncol.* **126**, 64–68. <https://doi.org/10.1016/j.ygyno.2012.04.023> (2012).
21. Chung, Y. S. *et al.* Prognostic value of complete metabolic response on (1)(8)F-FDG-PET/CT after three cycles of neoadjuvant chemotherapy in advanced high-grade serous ovarian cancer. *J. Gynecol. Oncol.* **33**, e28. <https://doi.org/10.3802/jgo.2022.33.e28> (2022).
22. Perrone, A. M. *et al.* Potential prognostic role of (18)F-FDG PET/CT in invasive epithelial ovarian cancer relapse. A preliminary study. *Cancers (Basel)* <https://doi.org/10.3390/cancers11050713> (2019).
23. Han, S., Kim, H., Kim, Y. J., Suh, C. H. & Woo, S. Prognostic value of volume-based metabolic parameters of (18)F-FDG PET/CT in ovarian cancer: A systematic review and meta-analysis. *Ann. Nucl. Med.* **32**, 669–677. <https://doi.org/10.1007/s12149-018-1289-1> (2018).
24. Chung, H. H. *et al.* Prognostic value of preoperative metabolic tumor volume and total lesion glycolysis in patients with epithelial ovarian cancer. *Ann. Surg. Oncol.* **19**, 1966–1972. <https://doi.org/10.1245/s10434-011-2153-x> (2012).
25. Lee, J. W. *et al.* The role of metabolic tumor volume and total lesion glycolysis on (1)(8)F-FDG PET/CT in the prognosis of epithelial ovarian cancer. *Eur. J. Nucl. Med. Mol. Imaging* **41**, 1898–1906. <https://doi.org/10.1007/s00259-014-2803-x> (2014).
26. Jacquet, P. & Sugarbaker, P. H. Clinical research methodologies in diagnosis and staging of patients with peritoneal carcinomatosis. *Cancer Treat. Res.* **82**, 359–374. https://doi.org/10.1007/978-1-4613-1247-5_23 (1996).
27. Mimoun, C. *et al.* Using a new diagnostic tool to predict lymph node metastasis in advanced epithelial ovarian cancer leads to simple lymphadenectomy decision rules: A multicentre study from the FRANCOGYN group. *PLoS ONE* **16**, e0258783. <https://doi.org/10.1371/journal.pone.0258783> (2021).
28. Crestani, A. *et al.* A pre-operative radiological score to predict lymph node metastasis in advanced epithelial ovarian cancer. *J. Gynecol. Obstet. Hum. Reprod.* **51**, 102464. <https://doi.org/10.1016/j.jogoh.2022.102464> (2022).
29. Yao, H. & Zhang, X. Prediction model of residual neural network for pathological confirmed lymph node metastasis of ovarian cancer. *Biomed. Res. Int.* **2022**, 9646846. <https://doi.org/10.1155/2022/9646846> (2022).
30. Oriuchi, N. *et al.* A new, accurate and conventional five-point method for quantitative evaluation of ascites using plain computed tomography in cancer patients. *Jpn. J. Clin. Oncol.* **35**, 386–390. <https://doi.org/10.1093/jco/hy1109> (2005).
31. Wang, X. & Lu, Z. Radiomics analysis of PET and CT components of (18)F-FDG PET/CT imaging for prediction of progression-free survival in advanced high-grade serous ovarian cancer. *Front. Oncol.* **11**, 638124. <https://doi.org/10.3389/fonc.2021.638124> (2021).
32. Beichel, R. R. *et al.* Semiautomated segmentation of head and neck cancers in 18F-FDG PET scans: A just-enough-interaction approach. *Med. Phys.* **43**, 2948–2964. <https://doi.org/10.1118/1.4948679> (2016).
33. Armstrong, D. K. *et al.* Ovarian cancer, version 2.2020, NCCN clinical practice guidelines in oncology. *J. Natl. Compr. Cancer Netw.* **19**, 191–226. <https://doi.org/10.6004/jnccn.2021.0007> (2021).
34. Svolgaard, O. *et al.* Lymphadenectomy in surgical stage I epithelial ovarian cancer. *Acta Obstet. Gynecol. Scand.* **93**, 256–260. <https://doi.org/10.1111/aogs.12322> (2014).
35. Grant, P., Sakellis, C. & Jacene, H. A. Gynecologic oncologic imaging with PET/CT. *Semin. Nucl. Med.* **44**, 461–478. <https://doi.org/10.1053/j.semnuclmed.2014.06.005> (2014).
36. Kitajima, K., Murakami, K., Yamasaki, E., Kaji, Y. & Sugimura, K. Accuracy of integrated FDG-PET/contrast-enhanced CT in detecting pelvic and paraortic lymph node metastasis in patients with uterine cancer. *Eur. Radiol.* **19**, 1529–1536. <https://doi.org/10.1007/s00330-008-1271-8> (2009).
37. Chen, H. Z. *et al.* The development and validation of a CT-based radiomics nomogram to preoperatively predict lymph node metastasis in high-grade serous ovarian cancer. *Front. Oncol.* **11**, 711648. <https://doi.org/10.3389/fonc.2021.711648> (2021).

Author contributions

Data collection: X.B.; Data analysis: X.B.; Manuscript writing: H.W.; Manuscript review: H.W. All the authors read and approved the final manuscript.

Competing interests

The authors declare no competing interests.

Additional information

Correspondence and requests for materials should be addressed to X.W.

Reprints and permissions information is available at www.nature.com/reprints.

Publisher's note Springer Nature remains neutral with regard to jurisdictional claims in published maps and institutional affiliations.



Open Access This article is licensed under a Creative Commons Attribution 4.0 International License, which permits use, sharing, adaptation, distribution and reproduction in any medium or format, as long as you give appropriate credit to the original author(s) and the source, provide a link to the Creative Commons licence, and indicate if changes were made. The images or other third party material in this article are included in the article's Creative Commons licence, unless indicated otherwise in a credit line to the material. If material is not included in the article's Creative Commons licence and your intended use is not permitted by statutory regulation or exceeds the permitted use, you will need to obtain permission directly from the copyright holder. To view a copy of this licence, visit <http://creativecommons.org/licenses/by/4.0/>.

© The Author(s) 2023